PHYSICAL REVIEW D **78,** 032012 (2008)

Inclusive radiative J/ψ decays

D. Besson,[1] T. K. Pedlar,[2] D. Cronin-Hennessy,[3] K. Y. Gao,[3] J. Hietala,[3] Y. Kubota,[3] T. Klein,[3] B. W. Lang,[3] R. Poling,[3] A. W. Scott,[3] P. Zweber,[3] S. Dobbs,[4] Z. Metreveli,[4] K. K. Seth,[4] A. Tomaradze,[4] J. Libby,[5] A. Powell,[5] G. Wilkinson,[5] K. M. Ecklund,[6] W. Love,[7] V. Savinov,[7] H. Mendez,[8] J. Y. Ge,[9] D. H. Miller,[9] I. P. J. Shipsey,[9] B. Xin,[9] G. S. Adams,[10] M. Anderson,[10] J. P. Cummings,[10] I. Danko,[10] D. Hu,[10] B. Moziak,[10] J. Napolitano,[10] Q. He,[11] J. Insler,[11] H. Muramatsu,[11] C. S. Park,[11] E. H. Thorndike,[11] F. Yang,[11] M. Artuso,[12] S. Blusk,[12] S. Khalil,[12] J. Li,[12] R. Mountain,[12] S. Nisar,[12] K. Randrianarivony,[12] N. Sultana,[12] T. Skwarnicki,[12] S. Stone,[12] J. C. Wang,[12] L. M. Zhang,[12] G. Bonvicini,[13] D. Cinabro,[13] M. Dubrovin,[13] A. Lincoln,[13] P. Naik,[14] J. Rademacker,[14] D. M. Asner,[15] K. W. Edwards,[15] J. Reed,[15] R. A. Briere,[16] T. Ferguson,[16] G. Tatishvili,[16] H. Vogel,[16] M. E. Watkins,[16] J. L. Rosner,[17] J. P. Alexander,[18] D. G. Cassel,[18] J. E. Duboscq,[18] R. Ehrlich,[18] L. Fields,[18] R. S. Galik,[18] L. Gibbons,[18] R. Gray,[18] S. W. Gray,[18] D. L. Hartill,[18] B. K. Heltsley,[18] D. Hertz,[18] J. M. Hunt,[18] J. Kandaswamy,[18] D. L. Kreinick,[18] V. E. Kuznetsov,[18] J. Ledoux,[18] H. Mahlke-Krüger,[18] D. Mohapatra,[18] P. U. E. Onyisi,[18] J. R. Patterson,[18] D. Peterson,[18] D. Riley,[18] A. Ryd,[18] A. J. Sadoff,[18] X. Shi,[18] S. Stroiney,[18] W. M. Sun,[18] T. Wilksen,[18] S. B. Athar,[19] R. Patel,[19] J. Yelton,[19] P. Rubin,[20] B. I. Eisenstein,[21] I. Karliner,[21] S. Mehrabyan,[21] N. Lowrey,[21] M. Selen,[21] E. J. White,[21] J. Wiss,[21] R. E. Mitchell,[22] and M. R. Shepherd[22]

(CLEO Collaboration)

[1]*University of Kansas, Lawrence, Kansas 66045, USA*
[2]*Luther College, Decorah, Iowa 52101, USA*
[3]*University of Minnesota, Minneapolis, Minnesota 55455, USA*
[4]*Northwestern University, Evanston, Illinois 60208, USA*
[5]*University of Oxford, Oxford OX1 3RH, United Kingdom*
[6]*State University of New York at Buffalo, Buffalo, New York 14260, USA*
[7]*University of Pittsburgh, Pittsburgh, Pennsylvania 15260, USA*
[8]*University of Puerto Rico, Mayaguez, Puerto Rico 00681*
[9]*Purdue University, West Lafayette, Indiana 47907, USA*
[10]*Rensselaer Polytechnic Institute, Troy, New York 12180, USA*
[11]*University of Rochester, Rochester, New York 14627, USA*
[12]*Syracuse University, Syracuse, New York 13244, USA*
[13]*Wayne State University, Detroit, Michigan 48202, USA*
[14]*University of Bristol, Bristol BS8 1TL, United Kingdom*
[15]*Carleton University, Ottawa, Ontario, Canada K1S 5B6*
[16]*Carnegie Mellon University, Pittsburgh, Pennsylvania 15213, USA*
[17]*Enrico Fermi Institute, University of Chicago, Chicago, Illinois 60637, USA*
[18]*Cornell University, Ithaca, New York 14853, USA*
[19]*University of Florida, Gainesville, Florida 32611, USA*
[20]*George Mason University, Fairfax, Virginia 22030, USA*
[21]*University of Illinois, Urbana-Champaign, Illinois 61801, USA*
[22]*Indiana University, Bloomington, Indiana 47405, USA*
(Received 7 June 2008; published 19 August 2008)

Using data taken with the CLEO-c detector at the Cornell Electron Storage Ring, we have investigated the direct-photon momentum spectrum in the decay $J/\psi(1S) \to \gamma gg$, via the ''tagged'' process: $e^+e^- \to \psi(2S)$; $\psi(2S) \to J/\psi\pi^+\pi^-$; $J/\psi \to \gamma + X$. Including contributions from two-body radiative decay processes, we find the ratio of the inclusive direct-photon branching fraction to that of the dominant three-gluon branching fraction $[R_\gamma = B(gg\gamma)/B(ggg)]$ to be $R_\gamma = 0.137 \pm 0.001 \pm 0.016 \pm 0.004$, where the errors shown are statistical, systematic, and the model-dependent uncertainty related to the extrapolation to zero photon energy. The shape of the scaled photon energy spectrum in $J/\psi \to gg\gamma$ is observed to be very similar to that of $\Upsilon \to gg\gamma$. The R_γ value obtained is roughly consistent with that expected by a simple quark-charge scaling $[R_\gamma \sim (q_c/q_b)^2]$ of the value determined at the $\Upsilon(1S)$, but somewhat higher than the value expected from the running of the strong coupling constant.

DOI: 10.1103/PhysRevD.78.032012 PACS numbers: 13.20.Gd, 13.20.−v, 13.40.Hq

 © 2008 The American Physical Society

I. INTRODUCTION

According to the Okubo-Zweig-Iizuka (OZI) rule, the preferred decay mode for charmonium would be through the production of a $D\bar{D}$ meson pair. For resonances below the $\psi(3770)$ however, this is not energetically possible. Thus the decay of the $J/\psi(1S)$ meson must proceed through OZI-suppressed channels. The three lowest-order decay modes of the J/ψ meson are the three-gluon (ggg), virtual photon (vacuum polarization) decays $J/\psi \to l^+l^-$ and $J/\psi \to q\bar{q}$ with a branching fraction given in terms of $\mathcal{R}_{\rm QCD} \equiv (e^+e^- \to q\bar{q})/(e^+e^- \to \mu^+\mu^-)$ as $\sim \mathcal{R}_{\rm QCD} \times \mathcal{B}(J/\psi \to l\bar{l})$, and two-gluon plus single-photon ($gg\gamma$) modes. Early theoretical work outlined expectations for the $gg\gamma$ decays of quarkonium [1]. For the $\psi(2S)$ and $\psi(3770)$ resonances, direct radiative transitions, both electromagnetic and hadronic, as well as decays to open charm [for the $\psi(3770)$], compete with these annihilation modes and therefore reduce the $gg\gamma$ branching fraction.

A. Inclusive total rate

Since $\Gamma_{ggg} \propto \alpha_s^3$ and $\Gamma_{gg\gamma} \propto \alpha_s^2\alpha_{em}$, the ratio of the branching fractions for the ggg and $gg\gamma$ decay modes for heavy quarkonia (also equal to the ratio of experimentally measured events $N_{gg\gamma}$ and N_{ggg}, respectively) is expected to follow [2]:

$$R_\gamma \equiv \frac{B_{gg\gamma}}{B_{ggg}} = \frac{N_{gg\gamma}}{N_{ggg}} = \frac{36}{5} q_c^2 \frac{\alpha_{em}}{\alpha_s}[1 + (2.2 \pm 0.6)\alpha_s/\pi]. \tag{1}$$

In this expression, the charm quark charge $q_c = 2/3$. Alternately, one can normalize to the well-measured dimuon channel and cancel the electromagnetic vertex: $B_{gg\gamma}/B_{\mu\mu} \propto \alpha_s^2$. In either case, one must define the momentum scale (Q^2) appropriate for this process. Although the value $Q^2 \sim M^2$ seems natural, the original prescription of Brodsky, Lepage, and Mackenzie ("BLM" [2]) gave $Q = 0.157M_{\Upsilon(1S)}$ for (the less-relativistic) $\Upsilon(1S) \to gg\gamma$. Alternative prescriptions for the appropriate value of Q^2 have also been suggested [3].

B. Energy and angular spectrum shapes

Calculations of the direct-photon energy spectrum were originally based on decays of orthopositronium into three photons, leading to the expectation that the J/ψ direct-photon energy spectrum should rise linearly with $z_\gamma(\equiv 2E_\gamma/M_{J/\psi})$ to the kinematic maximum ($z_\gamma \to 1$); phase space considerations lead to a slight enhancement at $z_\gamma = 1$ [4]. The angular distribution for the decay of a polarized vector into three massless vectors is, in principle, directly calculable. Thus, for direct radiative decays $J/\psi \to gg\gamma$, theory prescribes the correlation of z_γ with photon polar angle $\cos\theta_\gamma$, defined relative to the beam axis. Köller and Walsh considered the angular spectrum in detail [5], demonstrating that, if the parent is polarized along the beam axis, then, as the energy of the most energetic primary (photon or gluon) in $J/\psi \to \gamma gg$ or $J/\psi \to ggg$ approaches the beam energy, the event axis tends to increasingly align with the beam axis: $z_\gamma \to 1$ corresponds to $\alpha(z_\gamma) \to 1$ for an angular distribution specified as $dN/d\cos\theta_\gamma \sim 1 + \alpha(z_\gamma)\cos^2\theta_\gamma$. We note that, according to the Köller-Walsh prescription, the value of $\alpha(z_\gamma)$ for intermediate values, where most of the events occur, is relatively small (0.2). Only for $z > 0.9$ is the forward peaking of the photon angular distribution noticeable.

Previous analyses of the direct-photon spectrum in heavy quarkonium decay selected a fiducial angular region and integrated over $\cos\theta_\gamma$. In this analysis, we will take advantage of the expected correlations between $\cos\theta_\gamma$ and z_γ to improve the statistical precision of the extracted branching fraction. There is nevertheless still some model dependence in the extrapolation down to $z_\gamma \to 0$.

C. Previous work

Garcia and Soto (GS) [6] have performed the most recent calculation of the expected direct-photon spectrum in J/ψ decays, using an approach similar to that applied by the same authors for the case of $\Upsilon(1S) \to gg\gamma$ [7]. They model the endpoint region by combining nonrelativistic QCD (NRQCD) with soft collinear-effective theory (SCET), which facilitates calculation of the spectrum of the collinear gluons which occur as $z_\gamma \to 1$. Both color-octet and color-singlet contributions must be explicitly calculated and summed. The calculations are very sensitive to the handling of the octet contribution, and limit the momentum interval over which the theory is considered "reliable" to $0.4 \le z_\gamma \le 0.7$. At low energies (defined as $z_\gamma < 0.45$ for the case of the Υ), the so-called "fragmentation" photon component, due to photon radiation from final-state quarks, dominates.

Although inclusive radiative decays have received considerable experimental attention in the case of $b\bar{b}$ [8–13], the $c\bar{c}$ system has had only one prior measurement, by the MARK-II Collaboration in 1981 [14]. The MARK-II analysis, which utilized a calorimeter with resolution $\sigma_E/E \sim 0.12/\sqrt{E(\text{GeV})}$, resulted in a measurement for the inclusive partial branching fraction $\mathcal{B}(J/\psi \to \gamma X) = (4.1 \pm 0.8)\%$ limited to the range $z_\gamma > 0.6$. Although the authors do not explicitly quote a value for R_γ in their original reference, we can estimate an implied R_γ value assuming that $z_\gamma > 0.6$ constitutes 45% of the total spectrum (over the full $\cos\theta_\gamma$ range, based on results obtained for bottomonium), and using $\mathcal{R}_{\rm QCD}^{\rm ECM=3.1\ GeV} = 2.1$ and $\mathcal{B}_{\mu\mu} = 0.059$, such that $\mathcal{B}(ggg) + \mathcal{B}(gg\gamma) = 0.69$, yielding $R_\gamma = \mathcal{B}(gg\gamma)/\mathcal{B}(ggg) \sim (14.6 \pm 2.8)\%$. The MARK-II direct-photon spectrum peaked at $z_\gamma \sim 0.6$, inconsistent with expectations based on orthopositronium decay, but consistent with later bottomonium spectra.

II. DETECTOR AND EVENT SELECTION

The CLEO-c detector is essentially identical to the previous CLEO-III detector, with the exception of a modified innermost charged particle tracking system. Elements of the detector, as well as performance characteristics, are described in detail elsewhere [15–17]. Over the kinematic regime of interest to this analysis, the electromagnetic shower energy resolution is approximately 2%. The tracking system, ring imaging Cherenkov particle identification system, and electromagnetic calorimeter are all contained within a 1 Tesla superconducting solenoid.

In the absence of dedicated J/ψ data collected at CLEO-c, we use the cascade decay chain $\psi(2S) \to J/\psi\pi^+\pi^-$; $J/\psi \to gg\gamma$. Our data sample corresponds to approximately $27 \times 10^6 \psi(2S)$ decays [18] collected with the CLEO-c detector (our ''primary'' data sample, divided into two subsamples of data taken approximately three years apart); a much smaller (''secondary'') sample of slightly more than 10^6 $\psi(2S)$ decays collected with the CLEO-III detector is used for cross-checks. To ensure maximal efficiency, minimal event selection requirements are imposed on our candidate direct-photon sample—we require only that candidate events have at least two high-quality charged tracks (the two transition charged pion candidates) and no identified lepton charged tracks. Our lepton veto is effective in suppressing contamination from $J/\psi \to l^+l^-$. Monte Carlo simulations indicate that the trigger efficiency for events having two transition charged pions and a fiducially contained direct photon with $z_\gamma > 0.3$ is >99%.

III. ANALYSIS

To obtain R_γ, we must determine separately the number of direct-photon events and the number of three-gluon events. By using the decay chain $\psi(2S) \to J/\psi\pi^+\pi^-$; $J/\psi \to gg\gamma$, we circumvent initial state radiation backgrounds in our photon sample. The dominant background for $z_\gamma < 0.6$ is primarily from $\pi^0 \to \gamma\gamma$ and $\eta \to \gamma\gamma$. Photon selection requirements are essentially the same as those applied for our study of $\Upsilon \to gg\gamma$ [8]. Namely, we require showers detected in the electromagnetic calorimeter with energy deposition characteristics consistent with those expected for true photons, and which are well isolated from both charged tracks as well as other showers. Since the π^0 signal-to-noise ratio is high, we will, in contrast to our previous analysis, require that a candidate high-energy photon not combine with another high-quality photon to give an invariant mass within ± 6 MeV from the nominal π^0 mass m_π^0. However, we do not impose an η veto given the worse signal-to-noise ratio and the greater likelihood of incorrectly vetoing a true direct photon. The scatter plot of the raw candidate photon energy vs ''shifted'' dipion recoil mass (ECM $-$ $M_{\rm recoil}$) is shown in Fig. 1.

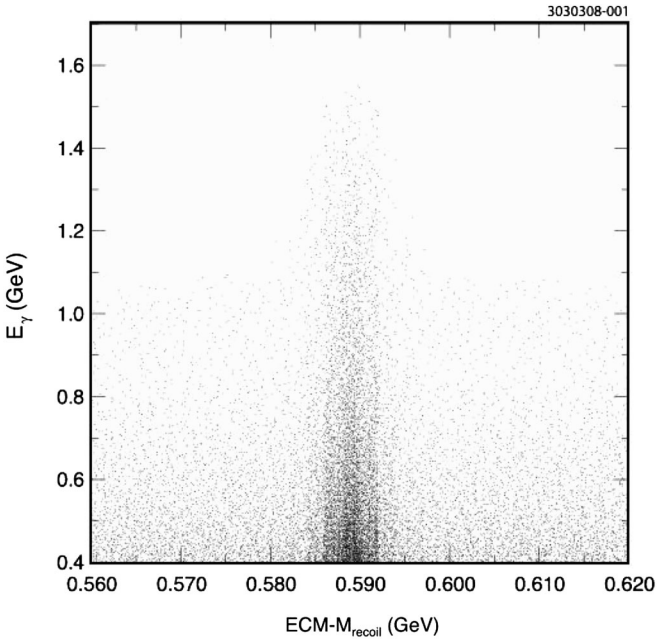

FIG. 1. Center-of-mass energy minus dipion recoil mass (horizontal) vs photon energy (vertical); $\psi(2S)$ data.

This spectrum includes contributions from each of the three main decay modes of the J/ψ: three-gluon, vacuum polarization, and direct-photon decay modes. Photons from nonresonant processes below the resonance, $e^+e^- \to q\bar{q}(\gamma)$, also contribute to this spectrum. However, since the charmonium peak cross section is a factor of 50 times larger than the continuum cross section, and we perform a dipion-sideband subtraction to obtain the tagged direct-photon spectrum from the J/ψ, we will, in what follows, ignore this continuum contribution. For the sideband subtraction, the signal region is defined as a dipion recoil region within ± 10 MeV$/c^2$ of the canonical J/ψ mass; sidebands are defined as the regions 10–40 MeV$/c^2$ from the canonical J/ψ mass.

Knowing the dipion four-vector allows us to work in the rest frame of the J/ψ itself; in what follows, unless otherwise indicated, the energy spectra presented for all signal as well as background photons correspond to this case.

IV. BACKGROUND PHOTON SUBTRACTION AND SIGNAL ESTIMATE

In the previous bottomonium analysis, two parametrizations of the background were used—one was based on the ''pseudophoton'' technique which has been used in three previous CLEO analyses [8,10,13], as well as the original MARK-II analysis, and the other used a simple exponential parametrization of the background under the direct-photon signal. The latter suffers from integrating over the correlations between $\cos\theta_\gamma$ and z_γ and is therefore not used in our current analysis. To model the production of π^0 and η daughter photons, redundant estimators were employed in

this analysis, which we detail below. Unlike the bottomonium analysis, we do not simulate $\omega \to \pi^0\gamma$ and $\eta' \to \gamma(\rho, \omega, \gamma)$ contributions. JETSET [19] indicates that these should be smaller than for the Υ. Numerically, the fraction of all $z_\gamma > 0.4$ photons having $\omega(\eta')$ parentage is 2.2% (0.8%) according to the LUND event generator, somewhat below our typical systematic errors. The nonphotonic contribution to our final candidate shower sample, due almost exclusively to K_L and $\bar{n}$ interactions in the calorimeter, is estimated from Monte Carlo simulations to be 1.5%. We note that, since the background shape is fixed during signal extraction, but the normalization is allowed to float, such nondirect-photon contamination is largely absorbed into the eventual background estimate.

A. Pseudophotons

As a first estimate of the nondirect-photon background, we took advantage of the expected similar kinematic distributions between charged and neutral pions, as dictated by isospin symmetry. Although isospin will break down both when there are decay processes which are not isospin symmetric in their final states ($J/\psi \to \gamma\eta$, $\eta \to \pi^0\pi^0\pi^0$) and when the available fragmentation phase space is comparable to M_π, in the intermediate-energy regime we expect isospin to be reliable. Over the kinematic regime relevant for this analysis, Monte Carlo studies indicate consistency (to within $\sim$5%) with the naive expectation that there should be half as many neutral pions as charged pions, with similar momentum-dependent angular distributions. However, unlike the case for the Υ, the region $z_\gamma \to 1$ has large contributions from two-body radiative decays. Specifically, the $\pi^0{:}\pi^\pm$ ratio grows in this regime due to decays such as $J/\psi \to \gamma\eta$ ($\eta \to 3\pi^0$) and $J/\psi \to \gamma\eta'$.

A pseudophoton spectrum $[d^2N/(dz_\gamma d\cos\theta_\gamma)]$ is constructed using charged tracks with particle identification information consistent with pions to model the spectra expected for π^0's and η's. In both cases, we use the Monte Carlo prescribed $\pi^0{:}\pi^\pm$ or $\eta{:}\pi^\pm$ ratios, taking into account the variation in these ratios with momentum. Momentum-dependent corrections are also applied to account for nonpion charged kaon, proton, and lepton fakes in our sample, as well as the finite charged track-finding efficiency. Each of these last two corrections are of order 5% and tend to offset each other. We invoke isospin in making the assumption that the momentum-dependent angular distribution of neutral pions follows that of charged pions. Our Monte Carlo generator indicates that the momentum-dependent angular distribution for η's is also similar to charged tracks. We simulate the two-body decays $\pi^0 \to \gamma\gamma$ and $\eta \to \gamma\gamma$ in the rest frame of the candidate π^0 or η parent and boost the daughter pseudophotons into the lab frame according to the (π^0 or η) momentum. The direct-photon-finding efficiency $\epsilon_\gamma(E_\gamma)$ is applied to each daughter pseudophoton to determine the likelihood that this photon will populate our candidate direct-photon spectrum. From Monte Carlo simulations, $\epsilon_\gamma \sim 0.85$ over the kinematic and geometric fiducial interval defined in this measurement. Finally, "found" pseudophotons are smeared in energy and angle by the known resolutions, and boosted into the candidate parent J/ψ frame.

To check our procedure, we have compared the data $\gamma\gamma$ invariant mass plot with the pseudophoton $\gamma\gamma$ invariant mass plot. To enhance statistics, we use all photons with $E_\gamma > 0.2$ GeV ($z_\gamma > 0.13$). At such relatively low photon energies, the number of accepted showers not having π^0 or η parentage is considerable, so we must also add to our $M_{\gamma\gamma}$ spectrum combinations of found π^0 or η daughter pseudophotons with "excess photons," using a Monte Carlo-based momentum-dependent factor. We obtain a level of agreement (better than 10%) consistent with our previous $\Upsilon(1S)$ analysis [8]. The comparison between our pseudophotons and data is shown in Fig. 2.

B. Background estimate from Monte Carlo simulations

Second, we use the Monte Carlo simulation of generic J/ψ decays, based on the JETSET 7.4 event generator, to provide an estimate of the background to the nondirect-photon signal, including all sources. This estimate implicitly includes all the corrections (photon efficiency, tracking efficiency and fake rates, $\pi^0{:}\pi^\pm$ ratio, hadronic showers, etc.) which must be explicitly evaluated in the previous

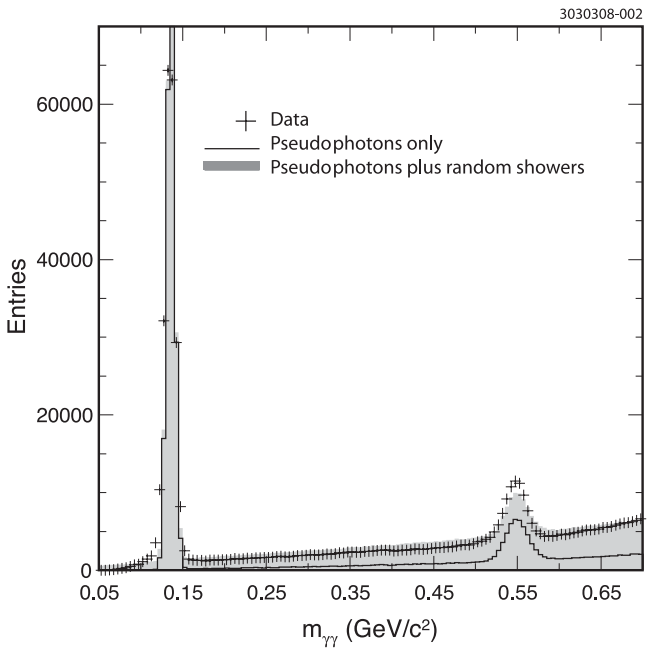

FIG. 2. Two-photon invariant mass combinations in data (crosses) vs pseudophoton simulation. The shaded histogram indicates pseudophoton simulation after adding combinations of simulated π^0 and η daughters with "excess" showers in data. Normalization is absolute.

approach. Therefore, no additional corrections are applied in this case.

C. Background using χ_{c0} decays

A third estimate of the background is obtained from decays of the $\chi_{c0}(3415)$, which is produced via the transition $\psi(2S) \to \chi_{c0}\gamma$ with the emission of a photon of energy 270 MeV. Since the χ_{c0} is relatively wide ($\Gamma \sim 10$ MeV), it has a relatively small radiative decay branching fraction to the J/ψ ($\mathcal{B} = 1.32 \pm 0.11\%$) and therefore dominantly decays via two-gluon intermediate states. To the extent that two-gluon fragmentation is similar to three-gluon fragmentation [20], we can therefore use the data photon background produced in association with an observed $\psi(2S) \to \chi_{c0}\gamma$ transition photon candidate to estimate the nondirect-photon background to the $\psi \to gg\gamma$ photon energy spectrum. Comparison of the charged track spectra for sideband-subtracted χ_{c0} vs J/ψ decays indicates that the kinematics of the former two-gluon decays are similar to the latter three-gluon decays in this case (Fig. 3).

To further suppress any possible $\chi_{c0} \to J/\psi\gamma$ cascade contamination, we veto events which contain a high-quality photon candidate of energy 322 ± 20 MeV. A signal region is defined around the 240–290 MeV transition photon energy range, and the photon energy spectrum in coincidence with the candidate transition photon (after sideband subtraction, with sidebands taken an additional 25 MeV on each side of the signal region) is then used as our last background estimator for our final fits.

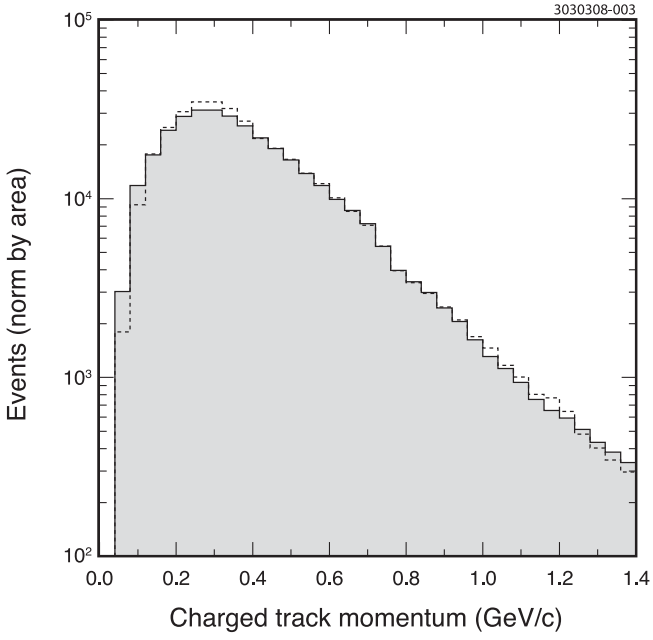

FIG. 3. Comparison of $\chi_{c0} \to \pi^{\pm}$ (shaded area) vs $J/\psi \to \pi^{\pm}$ (dashed line) inclusive charged track spectra.

D. Polarization of the parent J/ψ

In principle, the dipion transition can be either S- or D-wave, as allowed by parity conservation. The BES Collaboration has studied the angular distributions for this process [21] and found a best-fit value for the D-wave to S-wave amplitude of 0.18 ± 0.04. If the decay is all D-wave, then the $1 + a\cos^2\theta_\gamma$ distribution expected for two-body γ + pseudoscalar decays softens to $a \sim 0.07$ compared to $a = 1$ for S-wave. (We use the symbol a to designate the angular distribution of the radiative daughter photon specifically in two-body radiative decays.) Similarly, there is some uncertainty in the angular distribution of the direct-photon signal itself, characterized by the inclusive spectral parameter $\alpha(z_\gamma)$. To accommodate this, we have done fits varying values of both the two-body angular coefficient a and the inclusive direct-photon angular coefficient $\alpha(z_\gamma)$, and include the difference among them as a systematic error.

E. Fits and signal extraction

After imposing our event selection and photon selection criteria, we are left with the two-dimensional candidate direct-photon scaled energy vs polar angle distribution. We perform two-dimensional fits comprised of the following components: (a) the background, which is modeled either using the pseudophoton, Monte Carlo-based, or χ_{c0}-based backgrounds described above, (b) three two-body components of the direct-photon signal (to be included in the numerator of our final R_γ ratio), $\gamma\eta$ and $\gamma\eta'$, and a wide resonance which corresponds to $\gamma\eta(1440)$, with shapes determined from Monte Carlo simulation, and (c) a smooth signal component which has a shape in photon energy taken from our previous Upsilon decay measurement [8], and an angular distribution based on the Köller-Walsh prescription [5]. Ideally, we could avoid having to include a signal component. In such a case, the background subtraction would directly determine the true underlying signal. However, this can only be done if the background can be absolutely normalized with very high precision (much better than our $\sim$10% overall background normalization error). Unfortunately, the statistics of the fit are largely driven by the low-z_γ region, where the systematic uncertainty on the π^0 background is largest. Without inclusion of a signal component, the background normalization would increase to saturate the low-z_γ energy regime.

A comparison of the one-dimensional projections of the background dN/dz_γ spectra is shown in Fig. 4.

F. Validation of fit procedure using Monte Carlo simulations

For the Monte Carlo simulations, we can fit the signal plot with a combination of the tagged Monte Carlo simulation signal plus either the pseudophoton or the χ_{c0}-based background, and then check the signal normalization

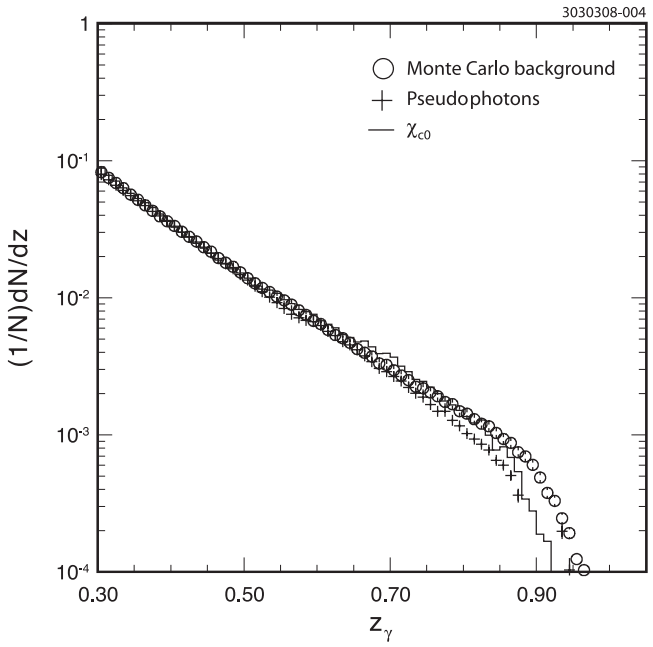

FIG. 4. Comparison of background photon $[(1/N)dN/dz_\gamma]$ spectra for the three subtraction schemes considered. Plus signs: pseudophoton background; histogram: χ_{c0} background; circles: Monte Carlo simulations of background.

against the known number of signal direct photons in the Monte Carlo simulations. The χ_{c0} background estimator results in a signal yield only 3% larger than the known number of Monte Carlo direct photons in the plot, while the pseudophoton background estimator underestimates the signal yield by ~15%. We note that the agreement between the signal yields obtained from these two backgrounds in data is typically within 3%. As discussed later, we nevertheless add an additional systematic error (6%) to reflect this discrepancy observed in simulation.

V. RESULTS

Figures 5–7 show sample fits over the kinematic region $z_\gamma > 0.3$ and $|\cos\theta_\gamma| < 0.8$, based on the pseudophoton model of the background, the Monte Carlo-based model of the background, and the χ_{c0}-based model of the background, respectively.

Positive residuals (data in one bin exceed sum of fit contributions) are shown in black; negative residuals (data in one bin are smaller than sum of fit contributions) are shown in white. Individual projections, onto the scaled photon energy and photon polar angle axes, for the three background models separately, are presented in Fig. 8. An overlay of the background-subtracted spectra, for the three background models employed, is shown in Fig. 9 for our primary data set. We observe reasonable agreement between the three spectra over most of the kinematic regime considered.

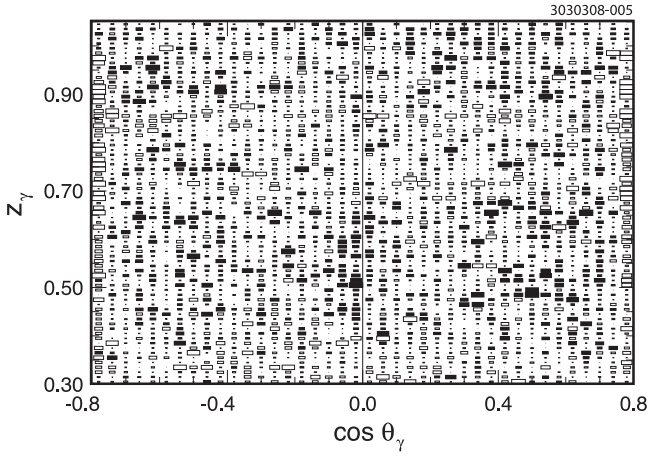

FIG. 5. Fit over the $z_\gamma > 0.3$, $|\cos\theta_\gamma| < 0.8$ kinematic region using pseudophoton background. Shown are normalized residuals, in units of statistical error per bin. Black: data > fit; white: data < fit. Excess at large values of $\cos\theta_\gamma$ is attributed to QED processes producing charged leptonic tracks at large dip angles, which are (incorrectly) used as input to the pseudophoton generator. This results in excess pseudophotons at high values of $\cos\theta_\gamma$.

Excluding electromagnetic transitions to other charmonium states, two-body radiative exclusive modes should be included in our total $gg\gamma$ yield. Decays into narrow η mesons have large enough branching fractions $[\mathcal{B}(\gamma\eta) = (9.8 \pm 1.0) \times 10^{-4}$ and $\mathcal{B}(\gamma\eta') = (4.71 \pm 0.27) \times 10^{-3}]$ so that they are clearly visible in the one-dimensional projection of the signal spectrum. Rather than fixing these contributions, we have allowed them to float and use the fitted area, corrected by efficiency, as a check of the overall procedure. We obtain estimates for the two-body branching fractions of $(8.1 \pm 0.6) \times 10^{-4}$ and

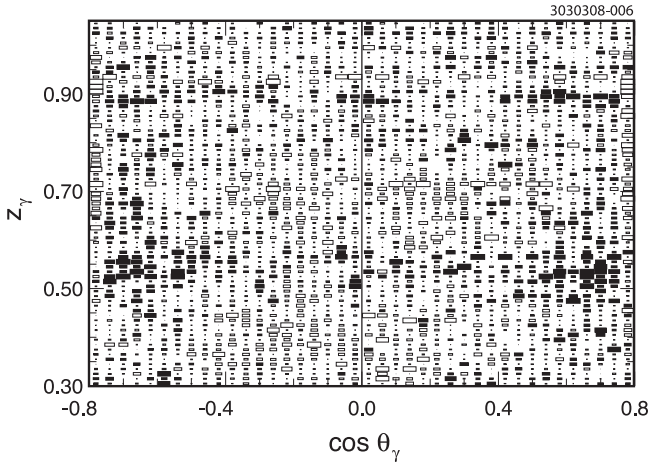

FIG. 6. Fit over $z_\gamma > 0.3$, $|\cos\theta_\gamma| < 0.8$ kinematic region, MC background. Black: data > fit; White: data < fit. Note apparent presence of extra two-body component in data, at $z_\gamma \approx 0.5$–0.55.

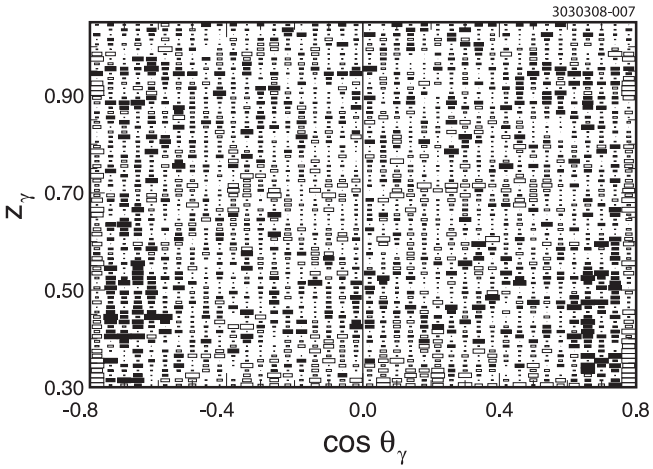

FIG. 7. Fit over the $z_\gamma > 0.3$, $|\cos\theta_\gamma| < 0.8$ kinematic region, χ_{c0} background. Black: data > fit; white: data < fit. We again note the apparent excess of data over background in the high-$\cos\theta_\gamma$ region around $0.4 < z_\gamma < 0.5$.

$(4.98 \pm 0.08) \times 10^{-3}$, respectively, for our primary data sample and $(8.8 \pm 2.1) \times 10^{-4}$ and $(5.4 \pm 0.4) \times 10^{-3}$ for our lower statistics, secondary data sample, where the errors presented are statistical only. Systematic errors for this coarse cross-check are likely to be at least as large.

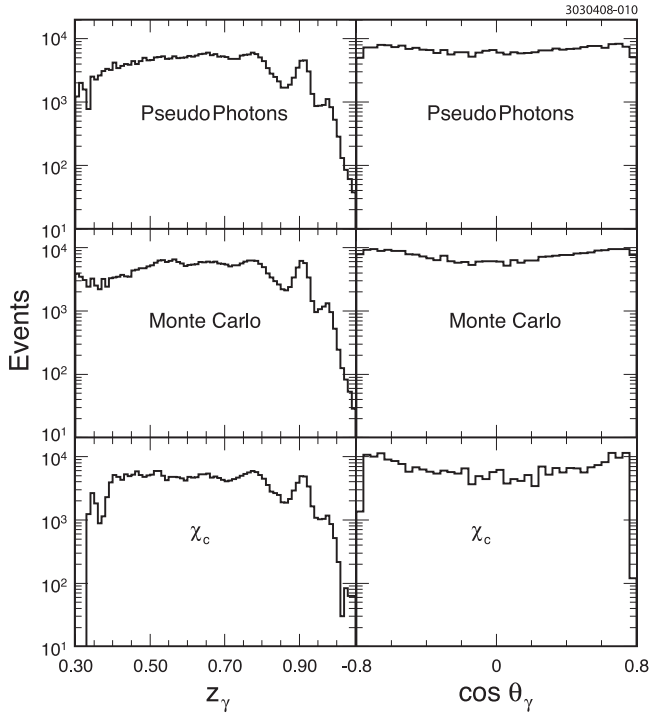

FIG. 8. Background-subtracted signal yield projections onto z_γ and $\cos\theta_\gamma$ axes, for the three photon background estimators used in this analysis.

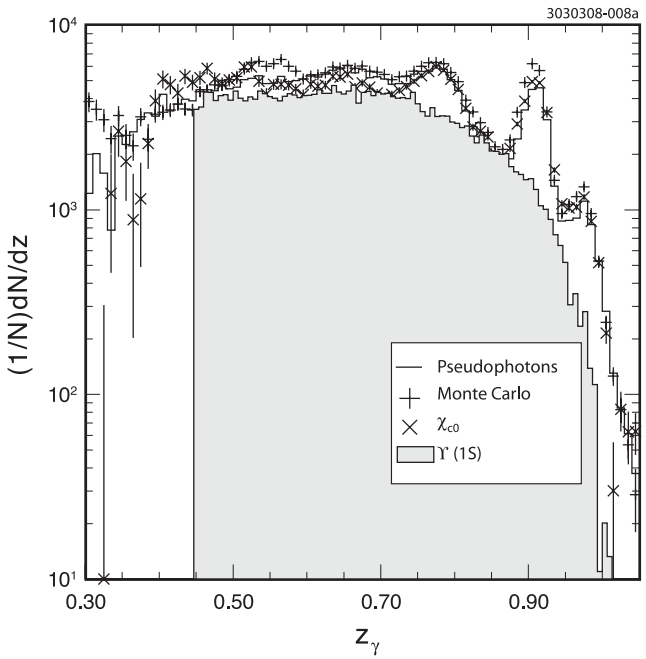

FIG. 9. $z_\gamma > 0.30$, $|\cos\theta_\gamma| < 0.8$, background-subtracted direct-photon energy spectra, using three different background subtraction schemes. Also overlaid (shaded histogram) is the experimental spectrum for the Υ spectrum, which was measured only to $z_\gamma = 0.45$.

VI. EXTRACTION OF R_γ

To determine R_γ, we calculate the ratio of true $N_{gg\gamma}$ (including radiative two-body decays) and N_{ggg} events [Eq. (1)]. The former quantity is the number of observed direct-photon candidates, corrected by the photon-finding efficiency and the kinematic acceptance. The latter quantity is the total number of $\psi(2S) \to J/\psi\pi^+\pi^-$ events estimated from our inclusive dipion recoil mass spectrum, minus contributions from $J/\psi \to gg\gamma$ (implicitly includ-

TABLE I. Summary of values of R_γ using varying kinematic regions for fits, different data sets, and background subtraction schemes. The first number is the primary subsample 1, and the second is the primary subsample 2. Numbers presented are simple averages of the values obtained using the three different background estimators. The number in parentheses following each average corresponds to the rms of the difference among the three background estimators and is therefore indicative of the (dominant) signal estimation systematic error. By comparison, the statistical errors returned by MINUIT from the fit (approximately the $\sqrt{N}$ errors on the total signal yield) are typically of order 1% for subsample 1 and 0.2% for subsample 2. Our final quoted R_γ result is a weighted average of the presented values.

	$\lvert\cos\theta_\gamma\rvert < 0.7$	$\lvert\cos\theta_\gamma\rvert < 0.8$
$z_\gamma > 0.30$	0.1367(88)/0.1398(78)	0.1338(97)/0.1371(85)
$z_\gamma > 0.45$	0.1320(110)/0.1362(94)	0.1332(89)/0.1403(98)

ing all two-body radiative components), $J/\psi \to l^+ l^-$, and $J/\psi \to q\bar{q}$. The two-track trigger efficiency is >99% for all these processes. The hadronic event reconstruction efficiency is also >99%; due to our lepton veto, the acceptance for dileptonic decays is less than 5%.

Table I shows the range of values obtained for two subsamples of the primary data, taken approximately three years apart (presented as ''subsample 1/subsample 2'') with varying definitions of the signal region.

VII. SYSTEMATIC ERRORS

We identify and estimate systematic errors in our R_γ determination as follows:

(1) The uncertainty in the S:D admixture of the dipion transition, in principle, affects the angular distribution ($\sim 1 + a\cos^2\theta_\gamma$) and therefore the acceptance for the two-body radiative component in our fits, as well as the angular distribution, and acceptance for the primary direct-photon signal component [$\sim 1 + \alpha(z_\gamma)\cos^2\theta_\gamma$]. Although both the S-wave and the dominant allowed D-wave transition amplitudes leave the daughter J/ψ polarized along the beam axis, we nevertheless allow for possible contributions due to D-wave amplitudes resulting in the daughter J/ψ polarized transverse to the beam axis. Varying a between 0.7 and 1.0 for the two-body modes results in a 1% change in the extracted direct-photon yield; varying $\alpha(z_\gamma)$ between the value prescribed by Köller-Walsh and $\alpha = 0$ for all photon momenta results in a 3% lower value for the extracted direct-photon yield. We attribute this to the larger saturation of the signal region by background which results when the signal photon angular distribution is taken to be flat in angle. We assume a systematic uncertainty of 3% due to this source.

(2) The uncertainty in the contribution to the signal due to nonphoton showers, based on Monte Carlo modeling of signal and background decays, is estimated to be 1.5%.

(3) Uncertainty in the number of three-gluon events is obtained by subtracting from the total number of dipion tags the number of $J/\psi \to \gamma^* \to q\bar{q}$ events, the number of signal $J/\psi \to \gamma^* \to gg\gamma$ events, and the number of $J/\psi \to \gamma^* \to l^+ l^-$ dileptonic decay events which pass our cuts. The statistical error on the branching fraction for $J/\psi \to \gamma^* \to q\bar{q}$ is very small ($\mathcal{B} = 13.50 \pm 0.30\%$) [22], as is the error on the dileptonic branching fraction ($5.94 \pm 0.06\%$). The fraction of dileptonic events which pass our cuts is also small ($\leq 5\%$), as is the statistical error on the number of $gg\gamma$ events in our sample. The total systematic error on our calculated ggg yield due to the non-ggg subtractions is largely due to the uncertainty in R_γ and is determined to be $\sim 2\%$.

(4) The trigger efficiency systematic error in the ratio is $\leq 1\%$.

(5) Background normalization and background shape uncertainty are evaluated by examining the agreement between the direct-photon yield obtained using the three different background estimators. We point out that these three techniques sample very different methods of background estimation. The χ_{c0} subtraction background estimate, e.g., is insensitive to the uncertainty in the overall photon-finding efficiency. Given the observed agreement across momentum, we infer that the pseudophoton technique is least likely to be sensitive to π^0/η modeling uncertainties.
However, we observe that the fits follow a generally consistent pattern. Although the data-driven fits (pseudophoton and using the χ_{c0} background) are generally consistent with each other at the 3% level, the average of the data-driven fits is consistently lower (by $\sim$15%) than the Monte Carlo-background subtracted spectra. The overall rms of the signals obtained using the three background estimators is 7% (see Table I), and we assign this value to the corresponding systematic error.

(6) The uncertainty in the absolute photon-finding efficiency is estimated at 2%.

(7) Sensitivity to the selection of signal and sideband regions in the dipion mass spectrum is estimated by increasing the nominal ''signal'' recoil mass interval by 25% and decreasing the nominal ''sideband'' recoil mass interval by 25%, indicating a systematic error <2%.

(8) The difference in our calculated value of R_γ between imposing vs not imposing the π^0 veto is found to be about 3%.

(9) For the pseudophoton subtraction only, the sensitivity to the assumed π^0:$\pi^\pm$ ratio was estimated by comparing the results based on the Monte Carlo-prescribed ratio vs a constant value of 0.5. This results in a variation of 3% in R_γ.

(10) Possible continuum QED contamination should be subtracted out via the dipion-sideband subtraction, although we do rely on Monte Carlo simulations to quantify the background from processes such as $\psi(2S) \to J/\psi\pi^+\pi^-$; $J/\psi \to l^+ l^-\gamma$. Our results with very strict QED suppression vs no QED suppression vary by 1%. We conservatively assign a 1% systematic error due to our uncertainty in this background.

(11) As described previously, we have compared the signal yield with the ''true'' signal yield using a Monte Carlo-only study, in which the number of simulated signal photons are known. Unfortunately, the JETSET 7.4 Monte Carlo simulated spectrum is entirely two-body and quasi-two-body, and does not

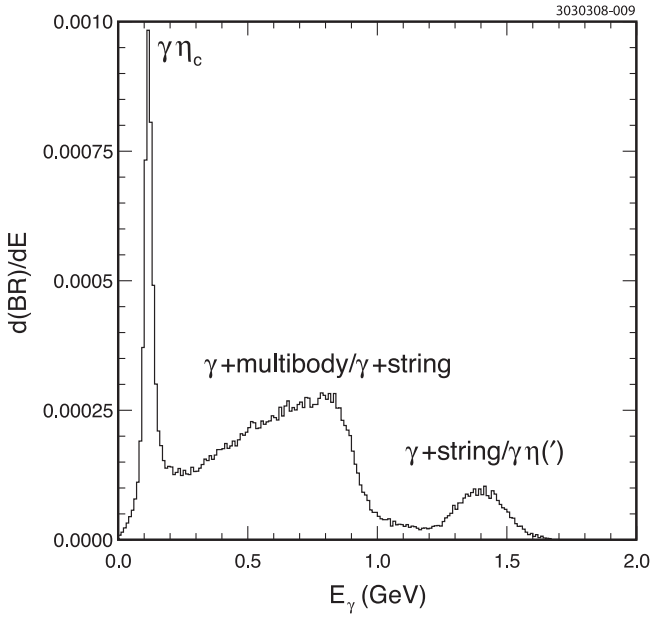

FIG. 10. Monte Carlo simulations of the J/ψ direct-photon momentum spectrum.

reproduce data well (Fig. 10). As outlined previously, we find that our average extracted signal yield is smaller than the true signal magnitude in Monte Carlo simulations by 6%, and conservatively (since this error likely is somewhat redundant with the systematic error assessed by the spread in R_γ values obtained using the three different subtraction schemes) include this as an additional systematic error.

A separate, additional systematic error must be included to account for the uncertainty in the extrapolation to $z_\gamma = 0$. For this, we compare the values obtained assuming a linear extrapolation from $z_\gamma = 0.3$ to $z_\gamma = 0$ vs an extrapolation based on the shape of the spectrum observed in the case of the Υ. The difference between the yields for these two extrapolations is $\leq 3\%$.

TABLE II. Systematic errors relevant to this analysis.

Source	Assigned systematic error
Photon angular distribution	3%
Nonphoton showers	1.5%
Number of three-gluon events	2%
Trigger efficiency	1%
Background subtraction	7%
Photon-finding efficiency	2%
J/ψ signal/sideband definition	2%
π^0 veto	3%
QED contamination	1%
Fitting systematics	6%
TOTAL	11.2%

TABLE III. Comparison with previous experiment. MARK-II errors are total. CLEO-c errors are statistical, systematic, and the uncertainty in the extrapolation to zero direct-photon momentum.

Experiment	R_γ
MARK-II [14]	0.041 ± 0.008 ($z_\gamma > 0.6$ only)
	0.146 ± 0.028 (all z_γ, estimated)
This measurement	$R_\gamma = 0.137 \pm 0.001 \pm 0.016 \pm 0.004$

Systematic errors are summarized in Table II.

Table III compares the results of this analysis with those obtained by previous experiments. Although the statistics are poorer, the older CLEO-III data (our cross-check sample) give results which are consistent with the CLEO-c results ($0.132 \pm 0.008 \pm 0.013$, where the first error is statistical and the second represents the spread in the measured values obtained using the three different background subtraction schemes).

VIII. IMPLICATIONS FOR α_s

Although the large relativistic corrections may render such an estimate unreliable, we can, nevertheless, calculate the value of α_s implied by our R_γ measurement, as shown in Fig. 11. Voloshin, in his recent review [23], estimates an expected branching fraction $\mathcal{B}(J/\psi \to gg\gamma) = 6.7\%$, using $\alpha_s(m_c) = 0.19$ and the known value of $\Gamma_{ee}(J/\psi)$. We can translate our value of R_γ into $\mathcal{B}$ by correcting for the non-ggg decays of the J/ψ, to obtain $\mathcal{B}(J/\psi \to gg\gamma) = 9.0 \pm 1.0\%$, considerably higher than Voloshin's estimate. We note that the earlier MARK-II result, extrapolated to the full kinematic regime, is also somewhat larger than Voloshin's estimate.

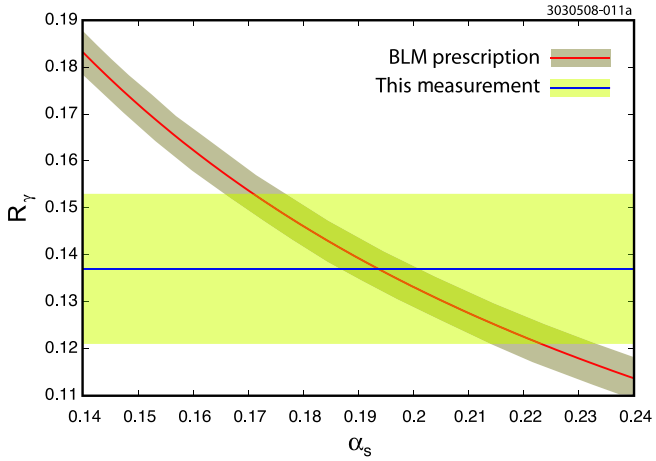

FIG. 11 (color online). The horizontal band indicates the R_γ central value and experimental uncertainties; the curve corresponds to the predicted α_s band (including theoretical errors), using the BLM prescription for $Q^2 = 0.157 M_{q\bar{q}}$.

IX. SUMMARY

We have extracted the direct-photon energy spectrum from J/ψ decays based on a two-dimensional fit procedure. Normalized to the dominant three-gluon mode of the J/ψ, and including two-body radiative decays, we obtain $R_\gamma = 0.137 \pm 0.001 \pm 0.016 \pm 0.004$. Although consistent with the one previous measurement, our direct-photon yield is somewhat higher than that expected by a simple extrapolation from results at the $\Upsilon(1S)$ ($R_\gamma = 2.78 \pm 0.08\%$, averaged over all previous measurements), taking into account the variation in $\alpha_s(Q^2)$.

ACKNOWLEDGMENTS

We gratefully acknowledge the effort of the CESR staff in providing us with excellent luminosity and running conditions. Shawn Henderson wrote initial versions of the computer codes used in this data analysis. We thank Xavier Garcia i Tormo and Joan Soto for illuminating discussions. D. Cronin-Hennessy and A. Ryd thank the A. P. Sloan Foundation. This work was supported by the National Science Foundation, the U.S. Department of Energy, the Natural Sciences and Engineering Research Council of Canada, and the U.K. Science and Technology Facilities Council.

[1] S. J. Brodsky, D. G. Coyne, T. A. DeGrand, and R. R. Horgan, Phys. Lett. **72B**, 227 (1977).
[2] S. J. Brodsky, G. P. Lepage, and P. B. Mackenzie, Phys. Rev. D **28**, 228 (1983).
[3] W. Kwong, P. Mackenzie, B. Rosenfeld, and J. Rosner, Phys. Rev. D **37**, 3210 (1988).
[4] S. J. Brodsky, T. A. DeGrand, R. R. Horgan, and D. G. Coyne, Phys. Lett. **73B**, 203 (1978).
[5] K. Köller and T. Walsh, Nucl. Phys. **B140**, 449 (1978).
[6] X. Garcia i Tormo and J. Soto, arXiv:hep-ph/0701030.
[7] X. Garcia i Tormo and J. Soto, Phys. Rev. D **72**, 054014 (2005).
[8] D. Besson *et al.* (CLEO Collaboration), Phys. Rev. D **74**, 012003 (2006).
[9] H. Albrecht *et al.* (ARGUS Collaboration), Z. Phys. C **54**, 13 (1992).
[10] S. E. Csorna *et al.* (CLEO Collaboration), Phys. Rev. Lett. **56**, 1222 (1986).
[11] H. Albrecht *et al.* (ARGUS Collaboration), Phys. Lett. B **199**, 291 (1987).
[12] A. Bizzeti *et al.* (Crystal Ball Collaboration), Phys. Lett. B **267**, 286 (1991).
[13] B. Nemati *et al.* (CLEO Collaboration), Phys. Rev. D **55**, 5273 (1997).
[14] D. L. Scharre *et al.* (MARK-II Collaboration), Phys. Rev. D **23**, 43 (1981).
[15] Y. Kubota *et al.* (CLEO Collaboration), Nucl. Instrum. Methods Phys. Res., Sect. A **320**, 66 (1992).
[16] D. Peterson *et al.*, Nucl. Instrum. Methods Phys. Res., Sect. A **478**, 142 (2002).
[17] M. Artuso *et al.*, Nucl. Instrum. Methods Phys. Res., Sect. A **502**, 91 (2003).
[18] H. Mendez *et al.* (CLEO Collaboration), Phys. Rev. D **78**, 011102(R) (2008).
[19] S. J. Sjostrand, LUND 7.3, Report No. CERN-TH-6488-92, 1992.
[20] M. S. Alam *et al.* (CLEO Collaboration), Phys. Rev. D **46**, 4822 (1992).
[21] J. Z. Bai *et al.* (BES Collaboration), Phys. Rev. D **62**, 032002 (2000).
[22] W.-M. Yao *et al.*, J. Phys. G **33**, 1 (2006).
[23] M. B. Voloshin, arXiv:0711.4556 [Prog. Part. Nucl. Phys. (to be published)].